Volume 21, No 2 | International Journal of Radiation Research, April 2023

Determination the dosimetric properties of scattering foil and scattering foil free electron beams in clinical linear accelerator

M. Zabihzadeh[1,2,3], Z. Sedaghat[2*], H. Shahbazian[3]

[1]Cancer Research Center, Ahvaz Jundishapur University of Medical Sciences, Ahvaz, Iran.
[2]Department of Medical Physics, School of Medicine, Ahvaz Jundishapur University of Medical Sciences, Ahvaz, Iran
[3]Department of Clinical Oncology, School of Medicine, Golestan Hospital, Ahvaz Jundishapur University of Medical Sciences, Ahvaz, Iran

► ***Original article***

Corresponding author:
Dr. Zeinab sedaghat,
E-mail:
z.sedaghat875@gmail.com

Received: August 2022
Final revised: September 2022
Accepted: October 2022

Int. J. Radiat. Res., April 2023; 21(2): 217-226

DOI: 10.52547/ijrr.21.2.6

Keywords: *Electron beam, linear accelerator, Monte Carlo calculation, radiotherapy, scattering foil, small field.*

ABSTRACT

***Background*:** Producing the ideal therapeutic electron beams from a clinical linear accelerator (Linac), is crucial to optimize dose delivery in radiotherapy. The aim of this study was to investigate the properties of electron beams with and without the scattering foil. ***Materials and Methods*:** Varian Linac 2100CD head was simulated by means of MCNPX-2.7 program. After validation with measured data, scattering foils were removed and then different dosimetric properties of 6 and 9 MeV electron beams such as depth dose percentage, dose profile, range, surface dose, dose rate and photon contamination were calculated and compared for field sizes ranging from 0.25×0.25 to 10×10 cm^2 in three states with primary and secondary scattering foil (SF), without primary scattering foil (PSFF) and without primary and secondary scattering foil (SFF). ***Results*:** By removing the scattering foils, dose rates and surface doses were increased more than 25 times in 0.25×0.25 cm^2 field, and in the bigger fields, it was less in 10×10 cm^2 field, almost 4 times and the photon contamination is reduced by 20% times in 0.25×0.25 cm^2 field. Also, Adjacent organs receive a lower dose, Because the dose profile curve was shrieked, it was almost 1cm in field 2×2 cm^2 and less than 1cm in other fields. The dose profile flatness was diminished in scattering foil-free (SFF) mode which is not crucial for the small fields. ***Conclusion*:** Removing scattering foil improves dosimetric properties of electron beams specially to treat the superficial tumors and for the small field radiotherapy.

INTRODUCTION

Electron therapy is widely used in the treatment of superficial and irregular malignant cancers such as skin, nose, eyelids or scalp, etc. Clinical electron beam has advantages of the uniformity of the dose in target volume and reduction of the dose to the distally located organs at risk (OARs) behind the target volume [1–3]. Deviation and scattering of the beam, contamination and penetration of the beam deeper than the target volume are the limiting factors for ideal radiation therapy [4–7]. The production of ideal electron beams poses a challenge for accelerator manufacturers to trade-offs between desirable (steep fall off, flatness) and undesirable features (photon contamination and applicator leakage) [8, 9] For this purpose, many studies investigated the components of the head of the device, including the presence or absence of falttering filters and scattering foils and applicators their dimensions and positions, and their materials [2, 10–13]. Akbarpour *et al.* simulated using mcnpx code an energy spoiler Perspex was modeled for degrading 4 MeV electron beam of Varian 2300 CD Linac. They found that using a 3mm spoiler would reduce the surface beam output to 77% and the surface dose for a 10mm filter would be 93%. D_{max} and R_P are reduced which is useful for skin treatment to minimize the dose to deeper tissues [14]. Titt *et al.* evaluated the Varian 2100 accelerator without filtering filter using Monte Carlo code. Their results showed that in the system without flattering the filter dose increased significantly, which reduced the out-of-field dose to patients due to reduced head-leakage dose [15]. Wakabayashi et al evaluated the safety and efficacy of a real-time variable shape rubber (STR) containing tungsten that can be placed on the patient's skin. They obtained experimentally and simulated electron beam profiles with STR placed on a low-melting-point alloy (LMA) water-equivalent phantom in the applicator (field sizes: 20 and 40 mm diameters), and The results showed that by using STR, the amount of photon pollution and R_{100} and Penumbras at the surface is reduced[16].

The scattering foil component implemented in

[DOI: 10.52547/ijrr.21.2.6]

linear accelerator (Linac) head was used to spread out the narrow electron beam to form different field sizes at varieties of surface-source distance (SSD) and maintains the flatness of dose profile at different depths [17, 18]. Present of scattering foil in the beam line attenuate and scatter the electron beam and decrease the electron fluence and constantly decrease the delivered dose at the depth of tumor. This indirectly increase the exposure time to deliver descripted dose to the target volume [19]. Furthermore, interaction of the electron beam with scattering foil produce bremsstrahlung photons that contaminate the impinging therapeutic electron beam [20]. More than 90% of contaminant photons is generated in Linac head and the scattering foil is responsible as the major contributing component. These contaminant photons due to their penetration perturbs the dose distribution of electron beam and deposit undesirable dose to healthy tissues and increase the side effects such as an increased risk of secondary cancer [21–23]. To solve this problem, some researchers investigated the beam parameters in removing the scattering foil. Eldib et al modeled and simulated scattering foil free electron beams using the Monte Carlo method and observed the dose was increased and a significant reduction of photon pollution by removing the primary scattering foil [24]. Other researchers reported a reduction of the Bremsstrahlung tail dose by a factor of 12.2, 6.9, 7.4, 7.4, and 8.3 for 6, 9, 12, 16, and 20 MeV beams, respectively, for 2×2 cm^2 by removing the scattering foil from the beam line [1].

The Monte Carlo method is widely used in radiation therapy due to its accuracy in calculating the interaction of neutrons, electrons, photons and heavy ion beams with materials. One of the methods to determine the character of the electron beam is to simulate the transfer of particles through the head treatment using the Monte Carlo technique [4, 25, 26], especially in small fields where there is a lack of electron lateral scatter equilibrium and more accurate dosimetry is required [3, 27, 28].

In previous studies, the complete quantitative data of the scattering foil affecting the dose distribution of the electron beam, which is very important for the modification of the linac head, has not been reported. Although, Sung simulated free foil scattering beam parameters of the Clinac iX using the BEAMnrc code and reported the R_{50} parameter and photon contamination for a 2×2 cm^2 field [29]. It seems that there may be differences in the dosimetry characteristics of different commercial linacs due to differences in the materials and geometries used in the head structure. To have full quantitative data about the scattering foil-free beam to evaluate its potential for the clinical applications, a Varian 2100CD photon linear accelerator was simulated using the MCNPX2.7 code. Dosimetric properties, including central axis absorbed dose, beam profiles, dose rate, photon and electron flux, and off –axis doses were calculated for different field sizes from 0.25×0.25 cm^2 to 10×10 cm^2.

MATERIALS AND METHODS

The PPDs and dose profiles of 6 and 9 MeV electron beams of 2100CD Varian Linac were measured by 0.13 cm^3 ionization chamber (PTW, Freiburg, Germany) with DOSE1 electrometer (Scanditronix -Wellhofer, Germany). The measurements were carried out at source to surface distance (SSD) of 100 cm in a IBA -Blue water phantom (IBA dosimetry Schwarzenbruck, Germany) with dimensions of 50 cm^3 and were processed by dosimetry software of RFAplus (Version 5.2, Scanditronix - Wellhofer, Germany). Each measurement was repeated three times with precision of ±0.2%. The international atomic energy agency (IAEA) protocol, TRS -398 were followed during dose measurements.

The head treatment components of 2100CD Varian Linac [30](Varian Medi-cal Systems, Palo Alto, CA, USA) for 6 and 9 MeV electron beams including primary collimator, beryllium window, primary and secondary scattering foil, ionization chamber, mirror, secondary collimator and applicator[31] was simulated by MCNPX-2.7 code [32]. The ENDF/B VIII.0 library based on ACE data was used to transport the radiation [33]. The geometry and composition of the materials of each component was were simulated based on manufacturer-provided information. The cut-off energy of the photons was considered to be 10 KeV and for the electrons 700 KeV. Percentage depth doses (PDDs) and dose profiles were calculated and compared for three modes of SF, PSFF, SFF in water phantom with dimensions of 50×50×50 cm^3 at SSD of 100 cm. The resolution for scoring of dose was considered as 1 mm. for validate the Linac head, the statistical uncertainty in PDDs and dose profiles compared to the measured data was considered less than 3% in 3 mm. Execution time was between 12 to 35 hours and was done in parallel with a virtual server (intel Xeon e5-2697 v3, 24 core).

After validation and calculation of PDDs and dose profiles, characteristics of produced electron beams such as R_P, R_{50}, E_0, E_{P0}, dose ratio and surface dose as well as particle flux and energy flux were calculated and compared to the standard mode of SF. The mean energy value ($\bar{E}_0$) and the most probable energy (E_{P0}) is calculated by equations (1) and (2) [34].

$$\bar{E}_0 = 2.33R_{50} \quad (1)$$

$$E_{po} = 0.22 + 1.98R_p + 0.0025R^2_p \quad (2)$$

Dose ratio was obtained by dividing the maximum dose of PSFF and SFF beams by the maximum dose of SF beam (equation 3).

[DOI: 10.52547/ijrr.21.2.6]

Dose Ratio =$Dmax_{PSFF\ or\ SFF}/Dmax_{SF}$ (3)

The amount of increased surface dose was obtained by dividing the surface dose of PSFF and SFF beams by the surface dose of SF beam (equation 4).

Increased surface dose = Surface dose (PSFF or SFF)/ Surface dose (SF) (4)

As well as particle flux and energy flux with F4, *F4 in all three modes was calculated. To calculate the Bremsstrahlung photon contamination of the radiotherapy device head components and air, an air layer with dimensions of 50×50×0.1 cm^3 on the surface of the phantom with zero photon importance (imp 0) was considered and the obtained PDD was compared with the previous case. A cylinder with a radius of 0.5 cm and a height of 1 mm in the center of the field and outside the field is considered to study the electron and photon flux in the state before and after removing the foils for the desired fields at 6 and 9 MeV. To investigate the electron and photon flux to the surface after the scattering foil, a cylinder with a radius of 0.5 cm and a length of 7 cm perpendicular to the central axis was considered and divided into voxels 0.1 mm thick. Relative dose errors (dose uncertainty per voxel) were less than 2% per simulation. OriginPro 2019 program was used to analyze the simulation data [35].

RESULTS

For the standard mode of SF, the incident electron beam with asymmetric Gaussian distribution with right full width at half maximum (FWHM) energy spectra of 2.5 and 2.2 MeV and left FWHM energy spectra of 1.5 and 2 MeV were used to gain the best agreement between the measurements and MC calculations for beams of 6 and 9 MeV, respectively [36, 37]. The results for benchmark the linac's head only for field size of 10×10 cm^2 are shown in figure 1. The maximum relative error of MC calculations was <1% and <0.5% for dose profile and PDD curves, respectively, that were less than the recommended value of 2%. The estimated gamma index (<1) confirms that the MC calculated and measured PDDs and dose profiles are in good agreement. These negligible differences may originate from the lack of information about the initial electron beam, as accelerator manufacturers rarely provide information about this important parameter.

The PDDs and dose profiles (figure 2) for 6 and 9 MeV electron beams normalized to the maximum dose for each fields were calculated for three modes of SF, PSFF and SFF in SDD = 100 cm.

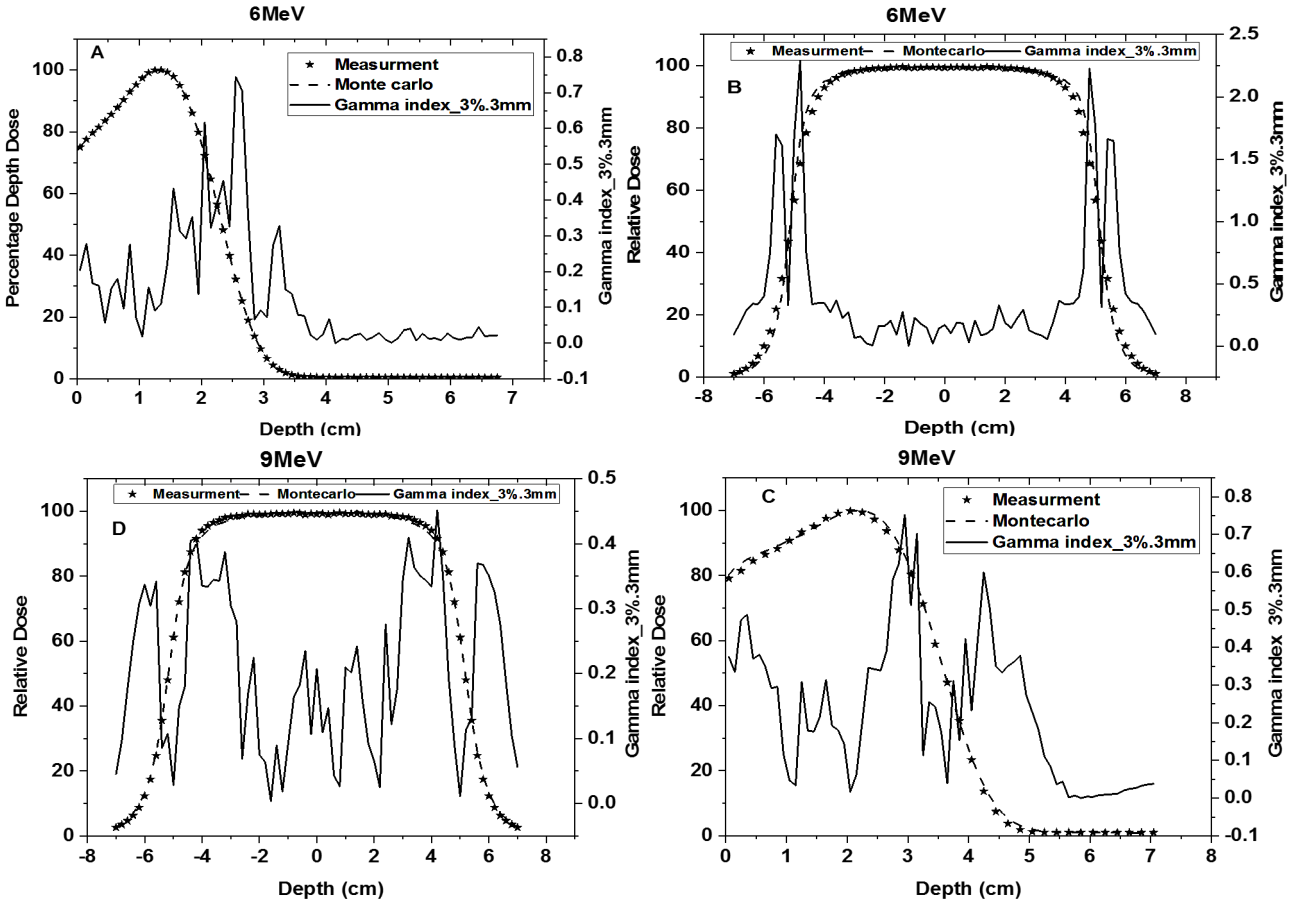

Figure 1. MC Calculated and measured PDD and dose profile: **(A)** and **(B)** for 6 MeV beam, and **(C)** and **(D)** for 9 MeV beam of 10 × 10 cm2 field size.

[DOI: 10.52547/ijrr.21.2.6]

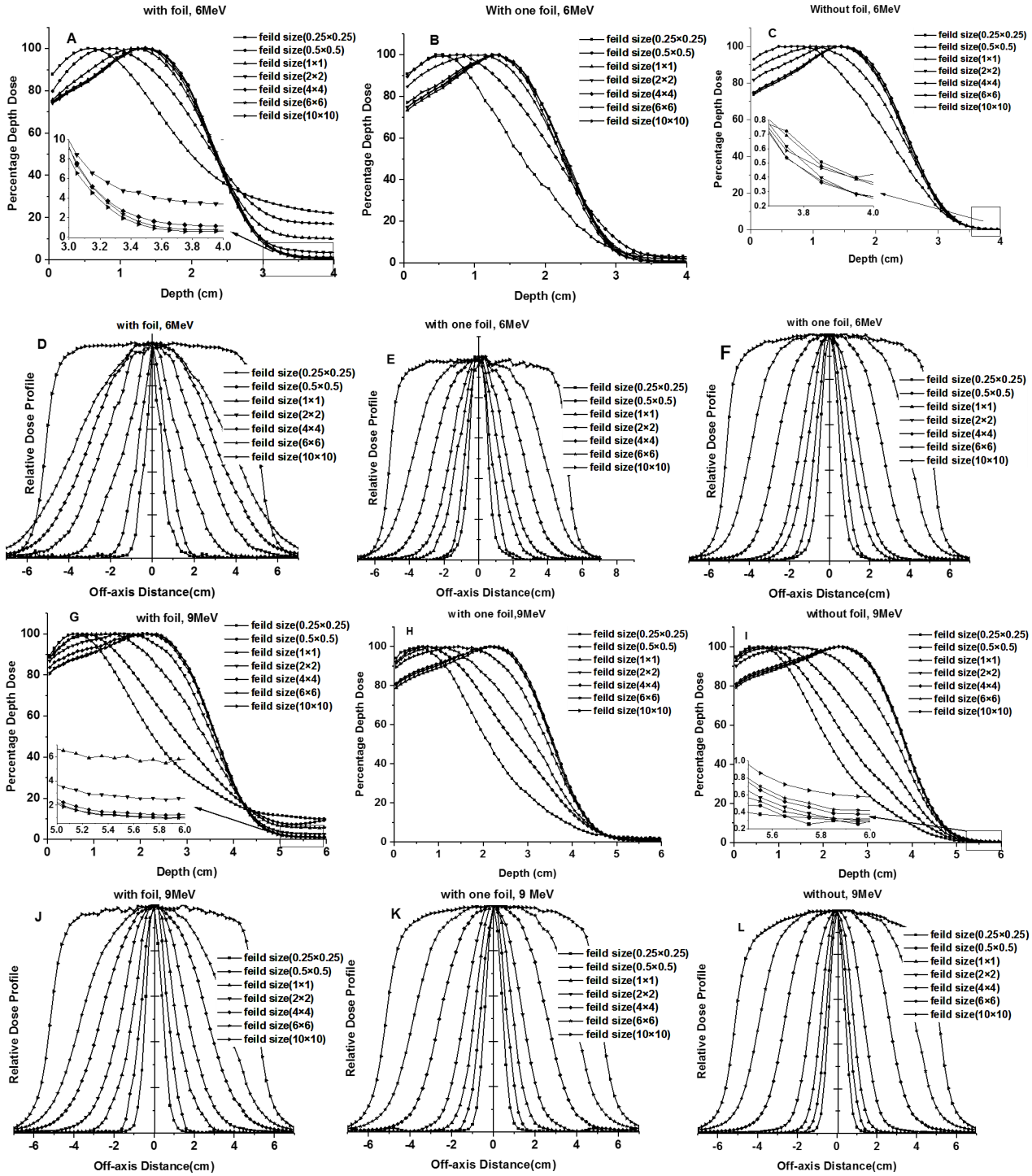

Figure 2. (A, B, C) PDD curve and **(D, E, F)** curve of electron beam dose profiles at energy 6 MeV and **(G, H, I)** PDD curve and **(J, K, L)** curve of electron beam dose profile fields for energy 9 MeV, Normalized to maximum dose depth, in the presence of scattering foil (with foil), in the absence of primary scattering foil (with one foil) and in the absence of primary and secondary scattering foil (without foil).

A comparison of PDDs and dose profiles normalized to the maximum dose of SF mode and profiles dose normalized to the maximum dose at energy 6 MeV for 0.25 × 0.25, 2 × 2 and 10 × 10 cm^2 fields can be seen in figure 3. After removing the scattering foil, the absorbed energy increased and the amount of this increase can be seen in the PDD curves.

The maximum dose range (R_{max}) and R_{50} has increased in fields larger than 2×2 cm^2 after the removal of scattering foils, while in fields smaller than 2×2 cm^2, it has become closer to the surface. The R_P obtained in SFF mode increased compared to the other two modes. R_{50} did not depend on the presence or absence of primary scattering foil and field size. Table 1 summarizes the characteristics of energy 6 MeV and table 2 summarizes the characteristics of energy 9 MeV.

[DOI: 10.52547/ijrr.21.2.6]

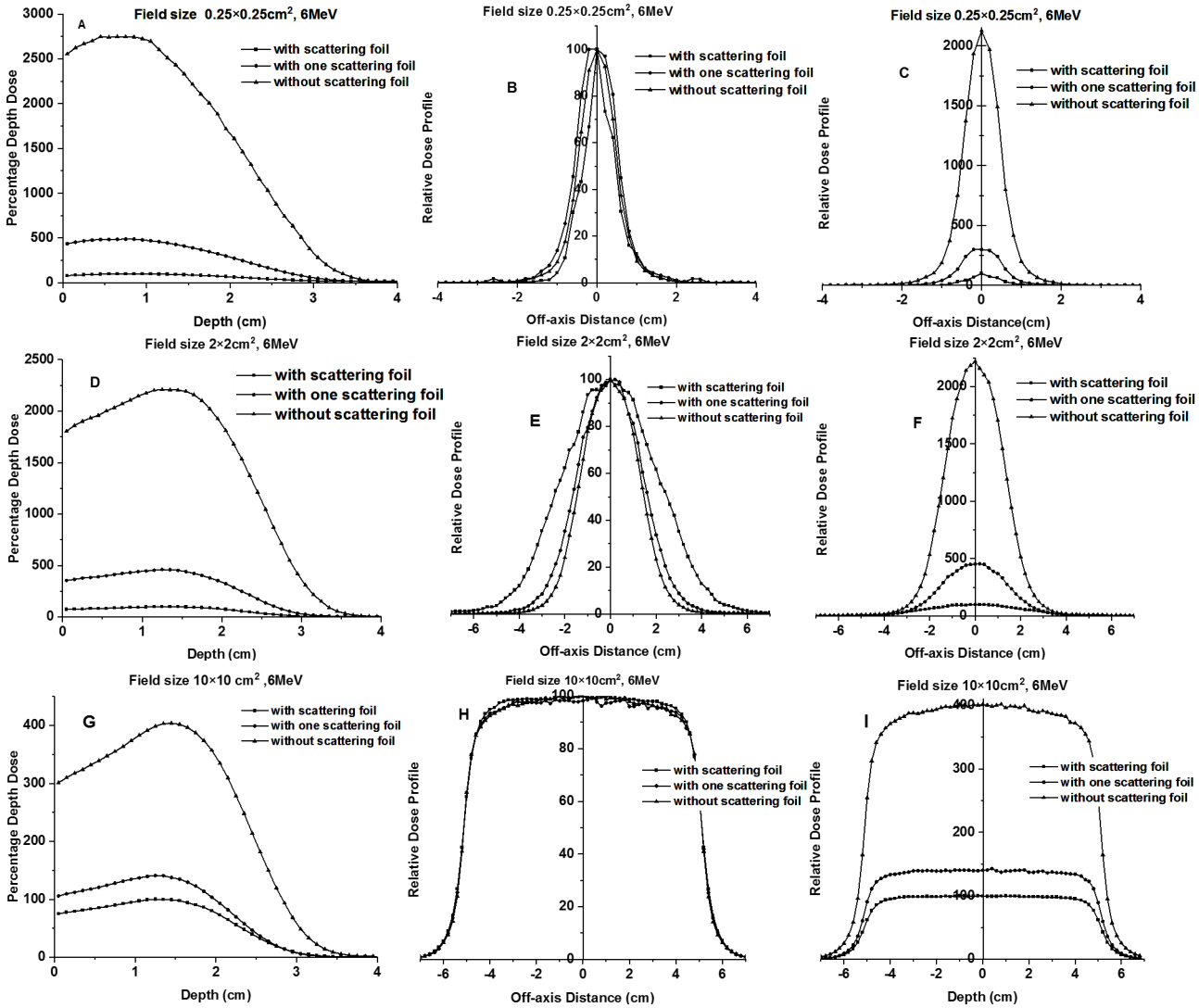

Figure 3. Comparison of **(A)** PDD curves and **(B)** profiles dose normalized to the maximum dose of SF mode, **(C)** profiles dose normalized to the maximum dose of SF mode of, **(D)** PDD curves and **(E)** profiles dose normalized to the maximum dose of SF mode, **(F)** profiles dose normalized to the maximum dose of SF mode, **(G)** PDD curves and **(H)** profiles dose normalized to the maximum dose of SF mode, **(I)** profiles dose normalized to the maximum dose of SF mode of in three modes (SF,PSFF,SFF) at 6 MeV.

Table 1. Beam characteristics of scattering foil free electron beams in the presence of scattering foil, in the absence of primary scattering foil and in the absence of primary and secondary scattering foil at energy 6 MeV.

Field size(cm^2), 6 MeV		R_{50}(cm)	R_P(cm)	R_{Max}(cm)	E_0	E_{po}
0.25×0.25	With Foil	2.59	1.96	0.55	6.03	4.11
	With one Foil	1.68	2.69	0.45	3.91	5.56
	Without Foil	1.70	2.96	0.55	3.96	6.10
0.5×0.5	With Foil	2.31	2.95	0.95	5.378	6.083
	With one Foil	2.16	3.05	0.85	5.04	6.28
	Without Foil	2.21	3.12	0.65	5.154	6.422
1×1	With Foil	2.34	2.97	1.25	5.443	6.123
	With one Foil	2.25	2.92	1.15	5.247	6.023
	Without Foil	2.43	3.19	0.95	5.66	6.562
2×2	With Foil	2.33	2.9	1.35	5.438	5.98
	With one Foil	2.30	2.9	1.25	5.368	5.98
	Without Foil	2.51	3.18	1.25	5.86	6.54
4×4	With Foil	2.35	2.93	1.25	5.47	6.043
	With one Foil	2.29	2.86	1.25	5.34	5.903
	Without Foil	2.52	3.14	1.45	5.881	6.462
6×6	With Foil	2.35	2.92	1.25	5.476	6.023
	With one Foil	2.27	2.83	1.35	5.298	5.84
	Without Foil	2.52	3.12	1.45	5.859	6.422
10×10	With Foil	2.32	2.88	1.25	5.41	5.94
	With one Foil	2.24	2.82	1.25	5.23	5.82
	Without Foil	2.49	3.1	1.45	5.79	6.382

Table 2. Beam characteristics of scattering foil free electron beams in the presence of scattering foil, in the absence of primary scattering foil and in the absence of primary and secondary scattering foil at energy 9 MeV.

Field size(cm^2), 9Mev		R_{50}(cm)	R_P(cm)	R_{Max}(cm)	E_0	E_{po}
0.25×0.25	With Foil	2.28	3.23	0.65	5.31	6.64
	With one Foil	2.15	3.13	0.55	5.0	6.44
	Without Foil	2.16	3.44	0.55	5.03	7.06
0.5×0.5	With Foil	2.86	4.31	0.85	6.67	8.80
	With one Foil	2.73	4.39	0.75	6.36	8.96
	Without Foil	2.61	4.62	0.65	6.072	9.42
1×1	With Foil	3.377	4.55	1.45	7.87	9.28
	With one Foil	3.17	4.42	0.75	7.39	9.02
	Without Foil	3.18	4.73	0.85	7.42	9.64
2×2	With Foil	3.55	4.4	1.45	8.27	8.98
	With one Foil	3.45	4.43	1.45	8.04	9.04
	Without Foil	3.383	4.67	1.25	7.88	9.52
4×4	With Foil	3.65	4.45	2.05	8.51	9.08
	With one Foil	3.58	4.39	2.15	8.34	8.96
	Without Foil	3.87	4.67	2.35	9.01	9.52
6×6	With Foil	3.63	4.41	2.15	8.46	9.0
	With one Foil	3.59	4.36	2.25	8.36	8.90
	Without Foil	3.88	4.65	2.35	9.03	9.48
10×10	With Foil	3.63	4.39	2.05	8.46	8.96
	With one Foil	3.57	4.34	2.15	8.32	8.86
	Without Foil	3.85	4.63	2.35	8.96	9.44

[DOI: 10.52547/ijrr.21.2.6]

As can been seen in figure 4 and table3, dose ratio was increased significantly in small fields for SFF beams. Dose ratio was 28.425 and 4.492 in 0.25 × 0.25 cm^2 field and 1.41 and 3.99 in 10 × 10 cm^2 field at 6 MeV for PSFF and SFF modes, respectively; the related data for 9 MeV beam was 22.59 and 4.28 and 4.33 and 1.55, respectively.

The increased surface dose was higher in SFF beams than PSFF. As can be seen from figure 5 and table 3, the increase of surface dose was 32.53, 4.65, 4.04 and 1.42 for SFF and PSFF and for 0.25×0.25 cm^2 and 10×10 cm^2 field at 6 MeV beam, respectively. For 9 MeV, it was 4.5 and 23.96 for 0.25×0.25 cm^2 field and 4.38 and 1.55 for 10×10 cm^2 field.

The dose in depths beyond the Rp is predominantly due to photon contamination. From figure 1, the amount of this unwanted dose from the photon contamination in fields smaller than 2×2 cm2 is greater than in larger fields. It is noticeable that Bremsstrahlung photon contamination is not just at the curve tail (which indicates a deep absorption beyond the range of electrons), this contamination is in all areas and causes an increase in the dose in the target area and before that. By removing the photon contamination by considering zero photon importance (imp: p 0) at surface of phantom, dose reduction due to diminish of contaminant photon after removing the scattering foils compare to standard field was calculated; the related data in the field of 10×10, 1×1, 0.5×0.5 and 0.25×0.25 cm^2 at energies of 6 can be seen in figure 6. This reduction rate is greater in small fields than in larger ones.

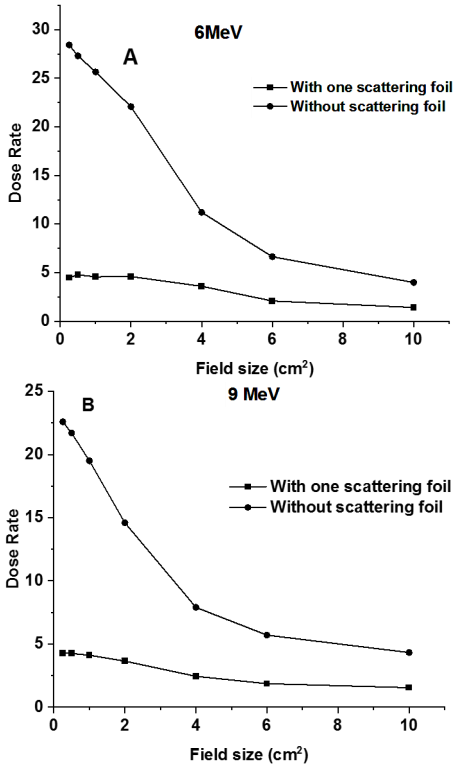

Figure 4. Dose ratio for PSFF and SFF modes; **(A)** 6 MeV, **(B)** 9 MeV.

Table 3. Surface dose and dose ratio, in the absence of primary scattering foil and in the absence of primary and secondary scattering foil at energy 6 and 9 MeV.

Field size(cm^2)		6MeV		9MeV	
		DoseRatio	SurfaceDose	DoseRatio	SurfaceDose
0.25×0.25	With one Foil	4.492	4.65	4.28	4.5
	Without Foil	28.425	32.53	22.59	23.96
0.5×0.5	With one Foil	4.78	5.45	4.26	4.46
	Without Foil	27.3	31.93	21.7	23.26
1×1	With one Foil	4.57	5.145	4.12	4.39
	Without Foil	25.64	29.86	19.5	21.22
2×2	With one Foil	4.6	4.8	3.65	3.75
	Without Foil	22.07	24.37	14.6	15.22
4×4	With one Foil	3.6	3.057	2.45	2.39
	Without Foil	11.2	11.39	7.9	7.77
6×6	With one Foil	2.09	2.06	1.87	1.83
	Without Foil	6.64	6.85	5.71	5.6
10×10	With one Foil	1.41	1.42	1.55	1.55
	Without Foil	3.99	4.04	4.33	4.38

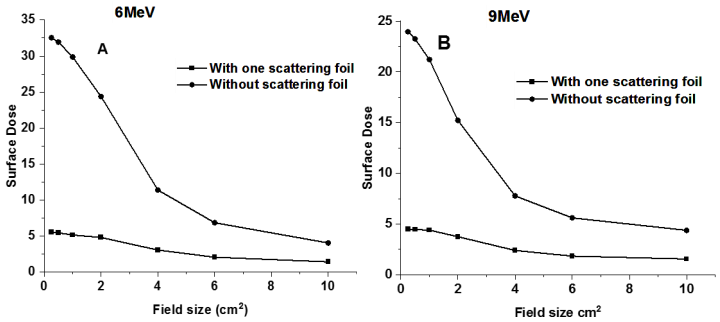

Figure 5. The increased surface dose for PSFF and SFF modes; **(A)** 6 MeV, **(B)** 9 MeV.

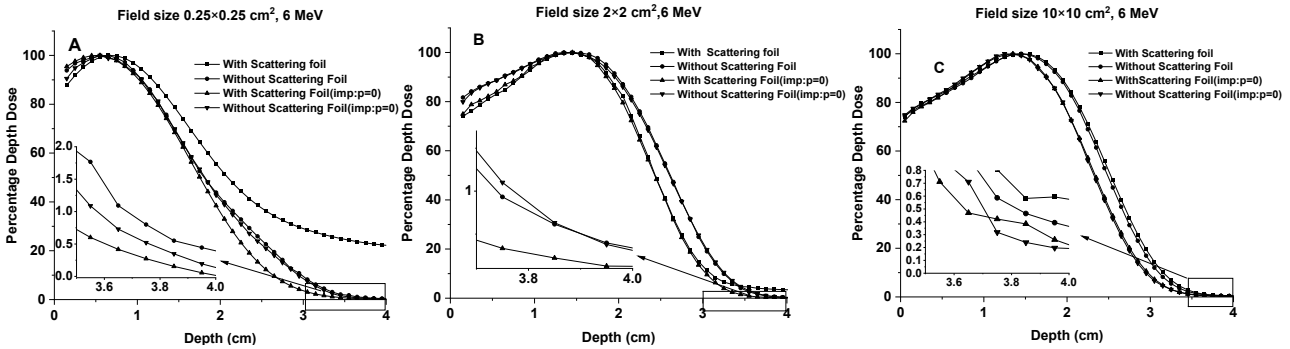

Figure 6. Effect of photon contamination on the Deep Dose Percentage (PDD) curve in **(A)** field 0.25 × 0.25 **(B)** field 2 × 2 and **(C)** field 10 × 10 for 6MeV electron beams.

[DOI: 10.52547/ijrr.21.2.6]

Figure 7 shows the flux of incident electron beams and photons to the surface under the scattering foil and it was observed that the presence of the scattering foil decreases the electron flux and increases the photon flux and is effective in their scattering. The incident electron and photon flux can be seen in the central axis and outside the fields of 0.25×0.25 cm² at energy 6 MeV, in the presence and without the presence of the scattering foil on the surface of the phantom in figure 8.

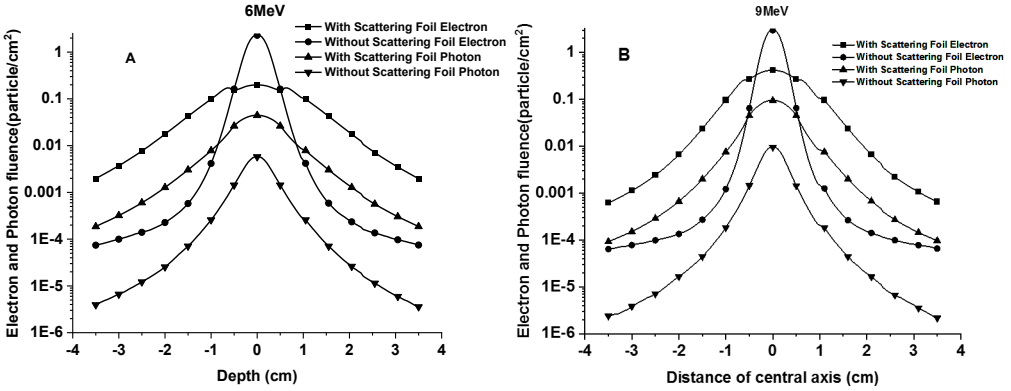

Figure 7. Electron and photon flux at downward surface of the scattering foil with and without the scattering foil; **(A)** at 6 MeV **(B)** at 9 MeV.

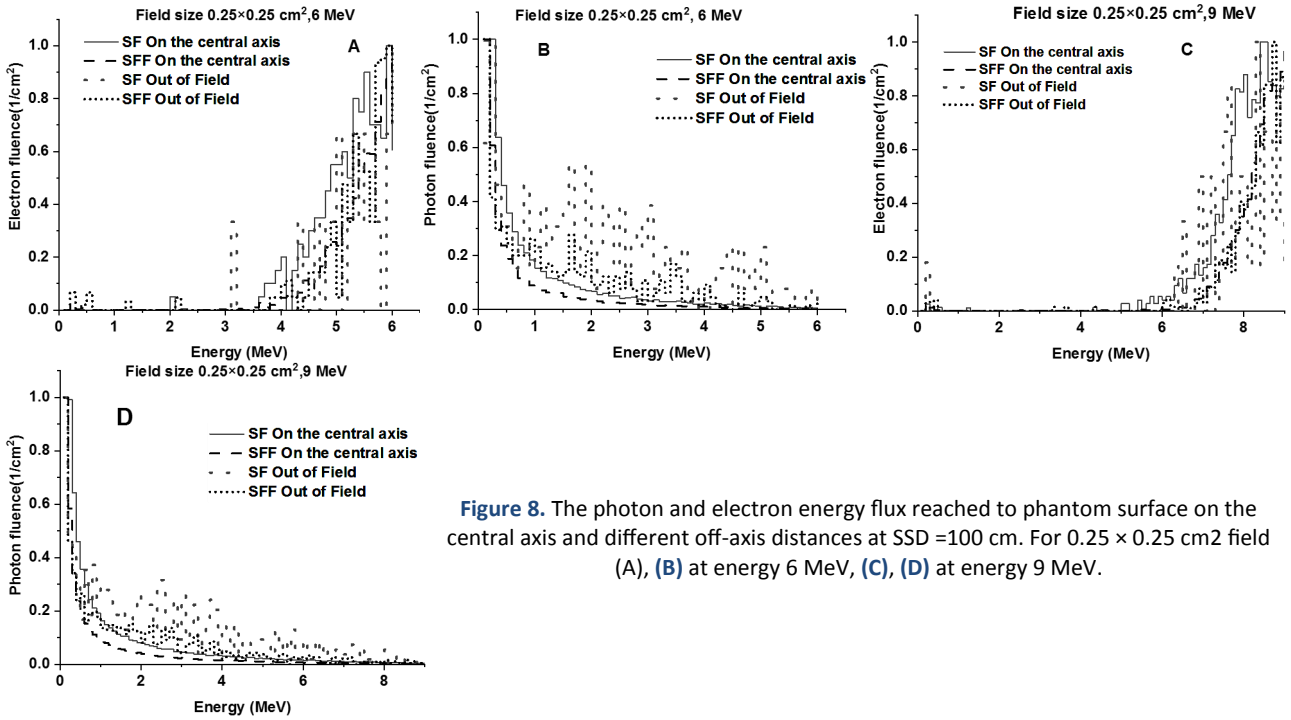

Figure 8. The photon and electron energy flux reached to phantom surface on the central axis and different off-axis distances at SSD =100 cm. For 0.25 × 0.25 cm2 field (A), **(B)** at energy 6 MeV, **(C)**, **(D)** at energy 9 MeV.

DISCUSSION

The PDD and profile curves for fields from 0.25×0.25 to 10×10 cm² are shown in figure 2. The shape of the profile was similar in all three cases (SF, PSFF, SFF) in fields smaller than 2, it was not smooth in all three cases, that is similar to the results was reported by Song *et al.* [29] and it was contradictory with Eldib *et al.*'s results [24]. Sung stated that the reason is due to the size of the field. We guessed that the way the mirror is placed in the shape of the dose profile is effective in small fields, so by removing the mirror in 0.5×0.5 cm² field in energies 6 and 9 MeV, it was observed that in SFF, swerving of the dose profile is reduced and becomes more symmetrical, which can be seen in figure 9. But the shrinkage of the profile dose in small fields will be suitable for the safety of organs at risk. This shrinkage in the SFF mode in fields 2×2 cm² is more than other fields, up to about 1 cm in the falloff part of the curve. At fields greater than 2×2 cm², the shrinkage decreases and as seen in figure 3 (H), this shrinkage is only at the edges of the field. This effect is less at 6MEV energy. As Eldib *et al.* removed the scattering foil and Vassilie *et al.* removed the flattering filters and showed that flat profiles have more changes at greater depth due to greater changes in beam quality with the distance from the central axis.[16,24] Comparison of PDD curves in figures 3A, D and G shows that The dose increased by removing the primary scattering foil (about 5 times in the 0.5 × 0.5 cm² field and about 1.2 times in the 10×10 cm² field), but by removing the primary and secondary foils, the increase reached about 25 times in the 0.5×0.5 cm² field and 4.5 times in the

[DOI: 10.52547/ijrr.21.2.6]

10×10 cm² field, and it can be due to the fact that the scattering foils block electrons with lower energy, while in the absence of that, these electrons hit a target.

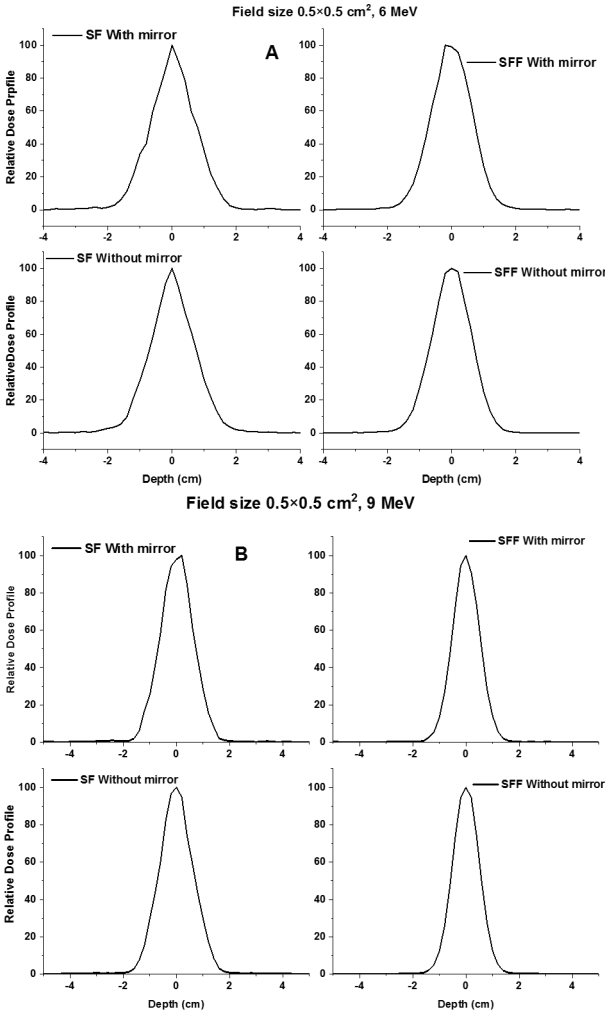

Figure 9. Dose profile symmetry with mirror removal in field at MeV **(A)** 6 and **(B)** 9 MeV energies.

From table 1, 2, R_{50} and R_{max} approaches the level in fields smaller than 4×4 cm², which can be because the contribution of electrons with higher energy is less or, due to the reduction of photon contamination, a lower dose will be delivered, which will result in an increase in the surface dose (figure 5, table 3), but this is not the case in fields 4×4 cm², 6×6 cm² and 10×10 cm². As shown by Eldib *et al.* [24] this result is inconsistent with Connells' results, which can be the reason for the presence of Few-Leaf Electron Collimator and applicator in their simulation after the foil removal [1]. By removing foils, the maximum dose range (R_P) increased, because the presence of foils weakens the electrons, so their penetration depth will be less compared to the presence of scattering foils [29]. According to formula (2), E_{P0} changes are the same as R_P and increases with the removal of scattering foils, and field 1×1 cm² range has the highest value and its value does not depend on the size of the field. The surface dose also has a significant increase, especially in fields smaller than 2, this advantage will be useful for surface treatments, but for the treatment of deep tumors, the skin dose should be considered. Increasing the dose ratio by removing the primary and secondary scattering foils has a significant increase in fields smaller than 2×2 cm². (table 3 and figure 4) By increasing the dose ratio, the treatment time will decrease, which is one of the advantages of removing the scattering foils. As it was reported that by removing the flattering filters, the surface dose and dose ratio increase[20,38].

It can be seen from figure 2 that by removing the scattering foil, the absorbed dose decreases in the tail of the curve. In the field of 0.5×0.5 cm², it decreases from 22% to below 1%, that is caused by the reduction of photon pollution at depths beyond the range (R_P) [1, 24]. The amount of contamination in smaller fields is higher than in larger fields, that seems to be caused by the collision of electrons with the edges of the collimator and the production of photons, which causes more flux of photons to enter the target and increases the dose [21]. In general, SFF beams have less contamination and its effect is greater for fields smaller than 2×2 cm². But it is worth noting that the Bremsstrahlung pollution is not only in the tail of the curve, but in all parts of the curve and causes an increase in the dose. This increased dose at the tumor site can be beneficial. It can be seen from figure 6 that the dose difference of the SF curve with and without considering the photon in the field of 0.25×0.25 cm2 at energy 6 increases to 28% and reaches 2% in the absence of scattering foils, which indicates the large contribution of scattering foils to photon pollution is compared to other components. Klein *et al.* investigated the amount of photon pollution by changing the design of the foils, and observed that the new double foil systems, that are thicker and disk -shape placed on the lower foils, increase the photon pollution (by a factor of 2) [9]. By changing the thickness and spacing of the scattering foils, Bieda *et al.* reported that the dose rate in the falloff section changes to a large extent, which indicates changes in the dose contribution due to the Bremsstrahlung component [39]. The changes in electron and photon flux of SF and SFF beams can be seen in figures 7 and 8.

Figure 7 shows the flux in the lateral distance from the central axis that reaches the surface under the scattering foil in the presence and absence of scattering foils. In the absence of scattered foils, the curve is narrower and the amount of electron flux is higher, that confirms the performance of the foils in scattering and weakening and blocking electrons, and also the decrease in the amount of flux also indicates the reduction of Bremsstrahlung contamination.

Figure 8 shows that the electron flux increases in the central axis after removing the foils, but the electron spectrum decreases, the electron flux

[DOI: 10.52547/ijrr.21.2.6]

outside the field decreases due to the reduction of scattering, and the photon flux in the central axis and outside the field due to collision Electrons are added to the scattering foils and produce bremsstrahlung. The absence of foil causes the electron flux to increase by 18.9 times in the field of 0.25×0.25 cm^2, but the photon flux is reduced by half, and in field 2×2 cm^2, this increases by 2.66 times for the electron flux and decreases by 0.53 times for the photon flux. After removing the flattering filter, the photon flux increases, according to the results reported by Mesbah *et al.*, the photon flux flatting filter free(FFF) increases by 1.4 times [20]. In another study, the flux rate was reported as 1.25. 35 These results are consistent with the increase of electron flux while the primary beam is electron [15].

CONCLUSION

By removing the scattering foils dose ratio and surface dose to the presence of foils significantly increased, photon contamination is reduced compared to the presence of foils, which can be desirable to prevent the increase in dose caused by the photons produced. Also, the penumbra was reduced due to the shrinkage of the dose profile, which means that the around organs are less exposed to dose absorption. due to the increase of the dose rate reduced the curing time. Therefore, foil removal in small fields and surface treatments will be more efficient.

ACKNOWLEDGEMENT

This report was a part of the MSc thesis by Zeinab Sedaghat. This research was funded by Vice-Chancellor for Research Affairs of Ahvaz Jundishapur University of Medical Sciences (Grant No. U-01057).

***Data availability statement*:** The data that support the findings of this study are available upon reasonable request from the authors.

***Conflict of Interest*:** The authors have no conflicts of interest to declare.

***Funding statement*:** This research received no specific grants from any funding agency in the public, commercial, or not-for-profit sectors.

***Ethics statement*:** There is no using animals and/or human subjects in this study.

***Author contributions*:** M. Zabihzadeh conceived and planned the study, performed the experiments, contributed to the interpretation of the results. Z. Sedaghat wrote and debugged the programs, arranged the data, contributed to the interpretation of the results and co-wrote the paper. H. Shahbazian analyzed and interpreted the data and measured experimental data.

REFERENCES

1. Connell T, Alexander A, Evans M, Seuntjens J (2012) An experimental feasibility study on the use of scattering foil free beams for modulated electron. *Phys Med Biol, **57**: 3259–3272*.
2. Ye S, Pareek PN, Spencer S, Duan J, Brezovich IA, Ye S, *et al.* (2005) Monte Carlo techniques for scattering foil design and dosimetry in total skin electron irradiations Monte Carlo techniques for scattering foil design and dosimetry in total skin electron irradiations. *Medical Physics, **32**: 1460*.
3. You A, Be M, In I (2017) The detector characteristics for output factor measurement of small field electron beams The Detector Characteristics for Output Factor Measurement of Small Field Electron Beams. *AIP Conference Proceedings, **1862**: 030072*.
4. Ma CM, Faddegon BA, Rogers DWO, Mackie TR (1997) Accurate characterization of Monte Carlo calculated electron beams for radiotherapy. *Med Phys, **24**(3): 401–16*.
5. Oh SA, Kang MK, Yea JW, Kim SK, Oh YK (2012) Study of the penumbra for high-energy photon beams with Gafchromic™ EBT2 films. *Journal of the Korean Physical Society, **60**(11): 1973–6*.
6. Mahmoudi A, Geraily G, Shirazi A, Hadisi nia T (2019) Penumbra reduction technique and factors affecting it in radiotherapy machines – Review study. *Radiation Physics and Chemistry, **157**: 22–7*.
7. Lax I and Brahme A (1980) Collimation of high energy electron beams Acta Oncologica. 19(3):199–207.
8. Klein EE, Li Z, Low DA (1996) Feasibility study of multileaf collimated electrons with a scattering foil based accelerator. *Radiotherapy and Oncology, **41**: 189–96*.
9. Klein E and Low D (1995) Changes in electron beam dosimetry with a new scattering foil-applicator system on a CL2100C. *Int Radiation Oncology Biol Phys, **32**(2): 483-490*.
10. Bennett LC and Vassiliev ON (2016) Examination of out-of-field dose and penumbral width of flattening filter free beams in medical linear accelerators. *Proceedings of NAPAC, Chicago, IL, USA 396–8*.
11. Mohammed M, Chakir E, Boukhal H, Mroan S, El Bardouni T (2017) Evaluation of the dosimetric characteristics of 6 MV flattened and unflattened photon beam. *Journal of King Saud University - Science, **29**(3): 371–9*.
12. Bjärngard BE, Piontek RW, Svensson GK (1976) Electron scattering and collimation system for a 12 MeV linear accelerator. *Medical Physics, **3**(3): 153–8*.
13. Kainz KK, Antolak JA, Almond PR, Bloch CD, Hogstrom KR (2005) Dual scattering foil design for poly-energetic electron beams. *Phys Med Biol, **50**: 755–767*.
14. Akbarpoor R, Khaledi N, Wang X, Samiei F (2019) U. Optimization of low-energy electron beam production for superficial cancer treatments by Monte Carlo code. *J Can Res Ther, **15**: 475-9*.
15. Titt U, Vassiliev ON, Pönisch F, Dong L, Liu H, Mohan R (2006) A flattening filter free photon treatment concept evaluation with Monte Carlo. *Medical Physics, **33**(6): 1595–602*.
16. Vassiliev ON, Titt U, Pönisch F, Kry SF, Mohan R, Gillin MT (2006) Dosimetric properties of photon beams from a flattening filter free clinical accelerator. *Physics in Medicine and Biology, **51**(7): 1907–17*.
17. Arjune B, Gilbert LD, Thekkumthala J (1991) Characteristic parameters of 6–21 MeV electron beams from a 21 MeV linear accelerator). *Medical Physics, **18**(4): 821–8*.
18. Olofsson L, Karlsson MG, Karlsson M (2005) Effects on electron beam penumbra using the photon MLC to reduce bremsstrahlung leakage for an add-on electron MLC. *Phys Med Biol, **50**: 1191–1203*.
19. Palta JR, Daftari IK, Ayyangar KM, Suntharalingam N (1990) Electron beam characteristics on a Philips SL25. *Medical Physics, **17** (1): 27–34*.
20. Mesbahi A, Mehnati P, Keshtkar A, Farajollahi A (2007) Dosimetric properties of a flattening filter-free 6-MV photon beam: a Monte Carlo study. *Radiat Med, **25**: 315–32421*.
21. Baghani HR and Aminafshar B (2019) In-field radiation contamination during intraoperative electron radiation therapy with a dedicated accelerator. *Applied Radiation and Isotopes, **155**: 108918*.
22. Ng J and Shuryak I (2014) Minimizing second cancer risk following radiotherapy: Current perspectives. *Cancer Management and Research, **7**: 1–11*.
23. Sorcini BB, Hyödynmaa S, Brahme A (1996) The role of phantom

[DOI: 10.52547/ijrr.21.2.6]

and treatment head generated bremsstrahlung in high-energy electron beam dosimetry. *Physics in Medicine and Biology,**41**(12): 2657–77*.
24. Eldib A, Jin L, Li J (2014) Investigation of the clinical potential of scattering foil free electron beams. P*hys Med Biol, **59**: 819–836*.
25. Laliæ D (2001) Comparison of measured and Monte Carlo calculated electron beam central axis depth dose in water. *Archive of Oncology, **9**(2): 83-7*.
26. Khaledi N, Aghamiri MR, Aslian H, Ameri A (2017) Tabulated square‐shaped source model for linear accelerator electron beam simulation. *J Can Res Ther, **13**: 69-79*.
27. Ulya S, Wibowo WE, Nuruddin N, Pawiro SA (2017) Dosimetric characteristics of gafchromic EBT3 film on small field electron beam. *J Phys, Conf. Ser. 851 012023*.
28. Keivan H, Shahbazi-Gahrouei D, Shanei A (2018) Evaluation of dosimetric characteristics of diodes and ionization chambers in small megavoltage photon field dosimetry. *Int J Radiat Res,**16**(3): 311-321*.
29. Sung W, Park JI, Kim J-i, Carlson J, Ye S-J, Park JM (2017) Monte Carlo simulation forscanning technique with scattering foil free electron beam: A proof of concept study. *PLoS ONE, **12**(5): e0177380*.
30. Varan Parto Darman, http://varanparto.com/fa/
31. Shimozato T, Okudaira K, Fuse H, Tabushi K (2013) Monte Carlo simulation and measurement of radiation leakage from applicators used in external electron radiotherapy. *Physica Medica, **29** (4): 388–396*.
32. Pelowitz DB. MCNPX TM User ' S Manual. 2008;
33. Lloyd CJ, Haeck W, Neudecker D, Kent Parsons D, White MC. LA-UR-18-24034: Release of ENDF/B-VIII.0-Based ACE Data Files. 2018;15. Available from: https://permalink.lanl.gov/object/tr?what=info:lanl-repo/lareport/LA-UR-18-24034
34. Khan FM and Gibbons JP (2014) Khan's the physics of radiation therapy. Lippincott Williams & Wilkins.
35. OriginLab - Origin and OriginPro - Data Analysis and Graphing Software https://www.originlab.com/
36. Kato T, Omachi S, Aso H (2002) Asymmetric Gaussian and its application to pattern recognition. Lecture Notes in Computer Science. *SSPR, **2396**: 405–13*.
37. Bj P and Kn T (2002) Influence of initial electron beam characteristics on Monte Carlo calculated absorbed dose distributions. *Phys Med Biol, **47**: 4019–4041*.
38. Sangeetha S and Sureka CS (2017) Comparison of Flattening Filter (FF) and Flattening-Filter-Free (FFF) 6 MV photon beam characteristics for small field dosimetry using EGSnrc Monte Carlo code. Radiation Physics and Chemistry. E*lsevier, **135**: 63–75*.
39. Bieda MR, Antolak JA, Hogstrom KR (2001) The effect of scattering foil parameters on electron-beam Monte Carlo calculations. *Med Phys, **12**(492): 2527–34*.

[DOI: 10.52547/ijrr.21.2.6]